

Lattice evidence for the family of decoupling solutions of Landau gauge Yang-Mills theory

André Sternbeck^{a,*}, Michael Müller-Preussker^b

^a*Institut für Theoretische Physik, Universität Regensburg, 93040 Regensburg, Germany*

^b*Institut für Physik, Humboldt-Universität zu Berlin, 12489 Berlin, Germany*

Abstract

We show that the low-momentum behavior of the lattice Landau-gauge gluon and ghost propagators is sensitive to the lowest non-trivial eigenvalue (λ_1) of the Faddeev-Popov operator. If the gauge fixing favors Gribov copies with small λ_1 the ghost dressing function rises more rapidly towards zero momentum than on copies with large λ_1 . This effect is seen for momenta below 1 GeV, and interestingly also for the gluon propagator at momenta below 0.2 GeV: For large λ_1 the gluon propagator levels out to a lower value at zero momentum than for small λ_1 . For momenta above 1 GeV no dependence on Gribov copies is seen. Although our data is only for a single lattice size and spacing, a comparison to the corresponding (decoupling) solutions from the DSE/FRGE study of Fischer, Maas and Pawłowski [Annals of Physics 324 (2009) 2408] yields already a good qualitative agreement.

Keywords: Landau gauge, gluon and ghost propagators, Gribov ambiguity, Faddeev-Popov eigenvalues

1. Introduction

Lattice calculations of the Landau-gauge gluon, ghost and quark propagators have attracted quite some interest during the last 15 years. Staunch supporters of pure lattice QCD (LQCD) may wonder about the enthusiasm with which such calculations have been performed and discussed in the past, in particular, as LQCD comes with the distinct advantage that one does not need to fix a gauge. This holds true, however, only as long as one is interested in gauge-invariant quantities. But besides LQCD there are also other (sometimes better suited) frameworks to tackle nonperturbative problems of QCD, and these require the exact knowledge of QCD's elementary two and three-point functions in Landau or other gauges.

Two continuum functional methods one has to mention here are the efforts to solve the infinite tower of Dyson-Schwinger equations (DSEs) of QCD or, likewise, the corresponding Functional Renormalization Group Equations (FRGEs) (see, e.g., the reviews [1–8] and references therein). Both these methods imply fixing a gauge (and often the Landau gauge is chosen for simplicity), but more importantly, these methods also require a truncation of the infinite system of equations to enable finding a numerical solution. These truncations are a potential source of error, which why corresponding (volume and continuum extrapolated) lattice results are so essential to render these truncations harmless or to even substitute parts of the DSE (or FRGE) solutions by (interpolated) nonperturbative data.

In what concerns the Landau-gauge gluon and ghost propagators, lattice results have helped much to improve truncations over the years. Currently, the continuum and lattice results overlap for a wide range of momenta, showing nice consistency among the so different approaches to QCD. Admittedly,

the currently used truncations are still not perfect, as seen, for example, for the gluon propagator whose DSE solutions differ from the corresponding lattice or FRGE results in the intermediate momentum regime (i.e., for momenta 0.5 – 3 GeV), whereas FRGE and lattice results agree much better there (see, e.g., Fig. 2 in [9]). But this situation will certainly improve, as it did in the past (see, e.g., [10] for recent progress).

Another regime that remains to be fully settled yet is the low (infrared) momentum regime. About the infrared behavior of the gluon and ghost propagators in Landau gauge there has been much dissent in the community and it is difficult to assess on the lattice also. Currently, all lattice studies agree upon a gluon propagator and ghost dressing function which are (most likely) finite in the zero-momentum limit (see, e.g., [11–19])¹. DSE and FRGE studies [20–23], on the other hand, assert that this infrared behavior is not unique, but depends on an additional (boundary) condition on the ghost dressing function at zero momentum, $J(0)$. Explicitly, in Refs. [22, 23], it is shown that for $J^{-1}(0) = 0$ one finds the so-called *scaling* behavior for the gluon and ghost propagators at low momentum, as it was first found in [24], while for finite $J(0)$, one finds a family of *decoupling* solutions for the DSEs and FRGEs, in qualitative agreement with DSE solutions proposed in the studies of Refs. [25–30], and with lattice results. For momenta above 1 GeV both types of solutions are practically indistinguishable. We interpret this ambiguity in the infrared as a remnant of the Gribov ambiguity of the Landau gauge condition, which is lifted by fixing $J^{-1}(0)$ to a constant.

In this letter we will show that a part of this one-parameter family of decoupling solutions can be seen on the lattice, at least qualitatively and as far as it is possible on a finite and

*Corresponding author

Email address: andre.sternbeck@ur.de (André Sternbeck)

¹Current lattice results for this regime are for finite lattice spacings and volumes only, and also the Gribov problem is only partially understood.

rather coarse lattice. Our approach also allows only for mild variations of the gluon and ghost propagators. Nonetheless, after outlining some technical details in the next section and a discussion about the distribution of the lowest non-trivial eigenvalue of the Faddeev-Popov (FP) operator, λ_1 , on different Gribov copies (Sect. 3), we will demonstrate in Sect. 4 that the decoupling-like behavior of the lattice gluon and ghost propagators can be changed by a (yet simple-minded implementation of a) constraint on λ_1 . Changes take place only in the low-momentum regime, but interestingly in a similar manner as one expects from the DSE/FRGE study [22], where a condition on $J(0)$ was used to change the low-momentum behavior². Specifically, we show that on Gribov copies with small λ_1 the ghost dressing function at low momenta rises more rapidly towards zero momentum than on copies with large λ_1 . Interestingly, a similar (though less pronounced) Gribov-copy effect is seen for the gluon propagator at low momentum. Qualitatively, our data thus resembles the change of the gluon and ghost dressing functions as expected from [22] for the corresponding decoupling solutions.³

Note that we still find Gribov copies by a maximization of the lattice Landau-gauge functional, but we are not interested in finding Gribov copies with large gauge-functional values, but on copies with comparably small (or large) λ_1 , irrespective of the functional value. On Gribov copies with large gauge-functional values we see both propagators to rise less rapidly towards zero momentum, consistent with what was found in the past [11, 31–34]

We should also mention here that similar effects were seen for the B -gauges by Maas [35]. For these gauges, one selects Gribov copies based on the ratio of the ghost dressing function at a small and a large lattice momentum on a particular copy. By construction the ghost dressing function in these gauges is then clearly enhanced or suppressed at low momenta. It remains to be seen if corresponding effects become clear also for the gluon propagator. The current data suggests, also this approach may reproduce a part of the family of decoupling solutions on the lattice [36, 37].

2. Simulation details

Our study is based on 80 thermalized gauge field configurations, generated with the usual heatbath thermalization and Wilson’s plaquette action for SU(2) lattice gauge theory. The lattice size is 56^4 and the coupling parameter $\beta = 2.3$. To reduce autocorrelations, configurations are separated by 2000 thermalization steps, each involving four over-relaxation and one heatbath step. For every configuration there are at least $N_{\text{copy}} = 210$ gauge-fixed (Gribov) copies, all fixed to lattice Landau gauge using an optimally-tuned over-relaxation algorithm for the gauge fixing that finds local maxima of the lattice

Landau gauge functional

$$F_U[g] = \frac{1}{4V} \sum_x \sum_{\mu=1}^4 \text{Tr} g_x U_{x\mu} g_{x+\hat{\mu}}^\dagger. \quad (1)$$

Here $U \equiv \{U_{x\hat{\mu}}\}$ denotes the gauge configuration and $g \equiv \{g_x\}$ one of the many gauge transformation fields fixing U to Landau gauge. To ensure these Gribov copies are all distinct, the gauge-fixing algorithm always started from a random gauge transformation field. Interestingly, for all these 80×210 gauge-fixing attempts only a few Gribov copies were found twice.

For every single Gribov copy we determine the lowest three (non-trivial) eigenvalues $0 < \lambda_1 < \lambda_2 < \lambda_3$ of the Faddeev-Popov (FP) operator using PARPACK [38]. In what follows, we will use λ_1 to classify copies: The Gribov copy with lowest λ_1 (considered for each configuration separately) is labeled *lowest copy* (lc), while the copy with the highest λ_1 we call *highest copy* (hc). The first generated copy, irrespective of λ_1 , gets the label *first copy* (fc). It represents an arbitrary (random) Gribov copy of a configuration. To compare with former lattice studies on the problem of Gribov copies we also reintroduce the label *best copy* (bc). It refers to that copy with the best (largest) gauge functional value $F_U[g]$ for a particular gauge configuration.

On those four sets of Gribov copies we calculate the SU(2) gluon and ghost propagators following standard recipes. That is, the gluon propagator is calculated for every lattice momentum using a fast Fourier transformation and the ghost propagator by using the plane-wave method for selected momenta. To accelerate the latter we use the preconditioned conjugate gradient algorithm of [11]. As a by-product of this calculation we also obtain the renormalization constant, \bar{Z}_1 , of the ghost-ghost-gluon (gh-gl) vertex in Landau gauge for zero incoming gluon momentum. For more details on lattice Landau gauge and the calculation of the propagators and \bar{Z}_1 the reader may refer to Refs. [11, 39–41] and references therein.

When quoting momenta in physical units we adopt the usual definition $ap_\mu(k_\mu) = 2 \sin(\pi k_\mu / L_\mu)$ with $k_\mu \in (-L_\mu/2, L_\mu/2]$ and $L_\mu \equiv 56$, assume for the string tension $\sqrt{\sigma} = 440 \text{ MeV}$ and use $\sigma a^2 = 0.145$ for $\beta = 2.3$ from Ref. [42], where a denotes the lattice spacing.

3. Distribution of λ_1

Before comparing the propagator data for the different types of Gribov copies, it is instructive to look at the distribution of λ_1 on all copies first. In Fig. 1 we show this eigenvalue distribution (in lattice units) for $N_{\text{cp}} = 210$ Gribov copies. There, the big panel shows it separately for each of the 80 gauge configurations and the small panel (on top) for all configurations together as a histogram. One sees that for most of the copies λ_1 takes values between 0.5×10^{-3} and 1.9×10^{-3} , mostly between 1.5×10^{-3} and 1.7×10^{-3} , but for some configurations there are also copies with an exceptionally small value for λ_1 , a value ($\lambda_1 < 10^{-4}$) far below the values found for the other copies. With our simple (brute-force) approach we are rather limited in finding more of these exceptional copies. The gauge-fixing and calculation of

²Note that in [22] the ghost dressing function is denoted G .

³We thank C. Fischer for providing us access to their (decoupling) solutions including those for smaller $J(0)$ not shown in [22].

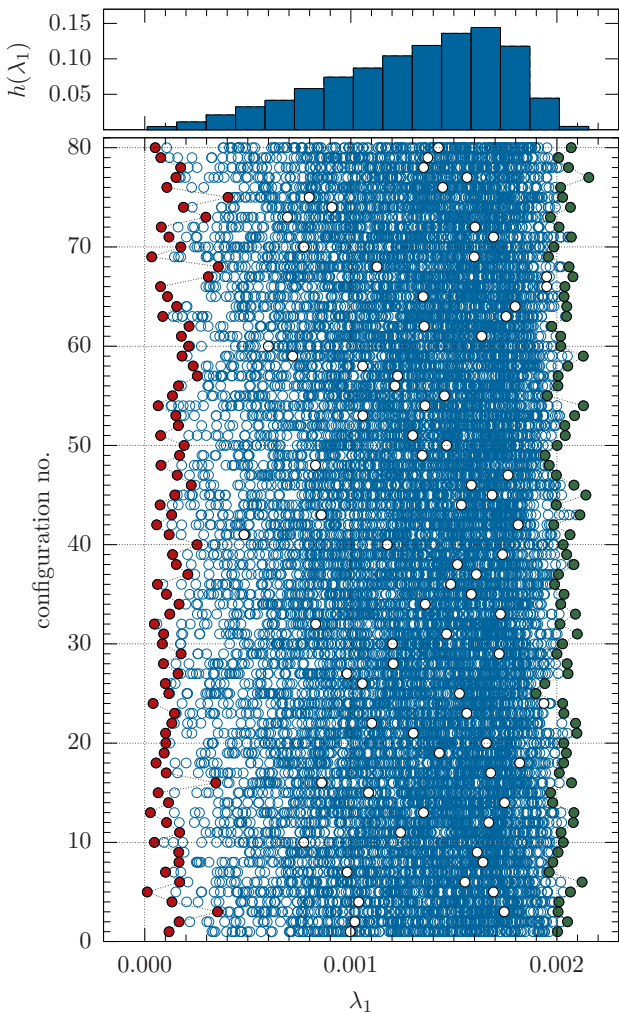


Figure 1: Distribution of λ_1 (in lattice units) for 210 Gribov copies, shown separately for 80 thermalized gauge configurations (ordinate). Full red (white, green) circles mark the eigenvalue on ℓc (fc , hc) copies. The small top panel shows as a histogram for λ_1 including all values found.

eigenvalues on a 56^4 lattice is computationally quite demanding, and a more sophisticated gauge-fixing algorithm—one which would automatically select that Gribov copy with the smallest (or at least with small) λ_1 —does not exist. But it would be interesting to know if for each configuration a Gribov copy with such an exceptionally small λ_1 exists.

For a few configurations we generated more than 210 Gribov copies. These allow us now to have a closer look at the distribution of λ_1 and to demonstrate that this number of copies is sufficient to resemble the distribution's shape for our lattice parameters ($\beta = 2.3$, 56^4).

Typical snapshots of this distribution for different N_{cp} are shown in Fig. 2, from left to right for three arbitrarily selected configurations. There, the middle panels illustrate how the range of λ_1 -values gets populated when increasing N_{cp} ; shown are distributions for $N_{\text{cp}} = 70$, 210, 420 and 500 Gribov copies. The top panels show the corresponding histograms, filled with the respective symbol color used in the middle panels. To ease

the comparison, these histograms are all normalized with respect to $N_{\text{cp}} = 420$.

From these histograms we see that the individual (configuration-wise) distributions of λ_1 are asymmetric and negatively skewed, similar to what we have just seen for the overall distribution in Fig. 1. Moreover, we see that at least 200 Gribov copies are needed to reach at an approximate shape for the distribution. This number of copies seems to be also sufficient (for the given lattice parameters) to find copies with either very small or very large λ_1 , even though it is unlikely that these copies are those with the respective smallest and largest λ_1 overall.

We are thus in a good position to analyze the correlation between λ_1 and the low-momentum behavior of the gluon and ghost propagator.

The attentive reader may have noticed the bottom panels of Fig. 2. These show correlation plots of λ_1 versus the gauge functional $F_U[g]$, always for the largest available number of Gribov copies ($N_{\text{cp}} = 420$ or 500) for the respective configuration. In former lattice studies on the infrared behavior of the gluon and ghost propagators (e.g., [15, 16, 33, 43]), gauge-fixing algorithms were often designed to find copies with comparably large $F_U[g]$, in the hope these copies are closer to the fundamental modular region than a set of random copies can be. Gribov copies which globally maximize the gauge functional are elements of the fundamental modular region, and it was argued [44–46] that in the continuum the common boundary of this region and the Gribov horizon (the set of Gribov copies with $\lambda_1 = 0$) is expected to dominate the path integral in the thermodynamic limit. This means that expectation values of correlation functions integrated over the fundamental modular region equal those integrated over the Gribov region [46]. It is however still open how these findings fit to the current lattice data, because in the Gribov-Zwanziger (GZ) approach the horizon condition also entails a gluon propagator (ghost dressing function) which vanishes (diverges) in the zero-momentum limit, which is not what is commonly seen on the lattice (see, e.g., [22, 37, 46, 47] for a more detailed discussion). These lattice results much better fit to the findings for the Refined-GZ approach [48] that also implements the horizon condition.

It is therefore interesting to check if small values for λ_1 are correlated with large values for $F_U[g]$. Looking at the scatter plots for $F_U[g]$ versus λ_1 (lower panels of Fig. 2), we find, however, there is no obvious correlation between them. There are copies with small λ_1 and small $F_U[g]$, but at the same time there are also copies with small λ_1 and large $F_U[g]$, and vice versa. Though, we see that on average highest copies tend to yield somewhat larger $F_U[g]$ values, in particular compared to random copies. This is consistent with our findings in [49].

4. λ_1 and the gluon and ghost propagators

Next we look at the correlation of λ_1 and the gluon and ghost propagator at low momenta. For the gluon propagator $D(k)$ [or its dressing function $Z(k) = p^2 D(k)$] there is actually no direct relationship between its momentum dependence and the spectrum of the FP operator, besides that it is gauge-dependent and

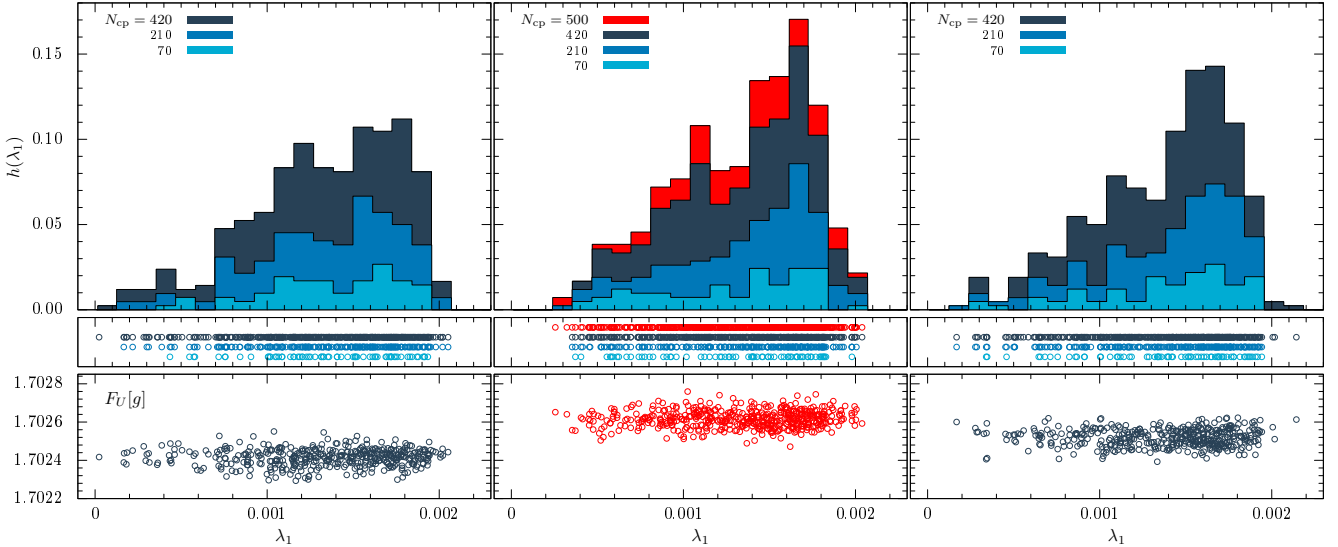


Figure 2: Top panels: histogram of the eigenvalue distribution of λ_1 for different numbers N_{cp} of Gribov copies. From left to right, each panel is for one gauge configuration. All histograms are normalized such that the sum of bars is one for $N_{\text{cp}} = 420$ copies. The middle panels show the corresponding scattering of λ_1 for the different N_{cp} , and the lower panels show scatter plots of λ_1 versus the gauge functional values $F_V[g]$ for the respective largest N_{cp} .

so may change if the lattice Landau gauge condition is supplemented by a condition on λ_1 .

The ghost propagator $G(k)$ [or its dressing function $J(k) = p^2 G(k)$], on the other hand, should be affected stronger. Given its spectral decomposition in $SU(2)$,

$$G(k) = \frac{1}{3} \sum_{i=1}^{3V-3} \frac{\vec{\Phi}_i(k) \cdot \vec{\Phi}_i(-k)}{\lambda_i}, \quad (2)$$

it is plausible that Gribov copies with very small λ_1 yield larger values for G than copies where λ_1 is comparably large, possibly even configuration-wise. Though this is not as simple as it seems at first sight, because λ_1 and the corresponding eigenfunction $\Phi_1(k)$ contribute only a minor fraction to $G(k)$ and this fraction even shrinks the larger the lattice momentum $a^2 p^2(k)$ (see Ref. [49], in particular Fig. 6 therein). However, from [50] (Fig. 1) we learn this fraction seems to increase with volume. That is, an anti-correlation of λ_1 and G is suggested.

For a few gauge configurations we have data for the gluon and ghost propagator for all Gribov copies. It allows us to check if there is a direct correlation between λ_1 and the gluon and ghost propagator at low momenta, comparing different Gribov copies of the same configuration. Looking at this data reveals, however, no immediate correlation: A Gribov copy with a smaller λ_1 not necessarily yields a larger ghost propagator than a copy with a somewhat larger λ_1 . Similar we find for the gluon propagator.

Nonetheless, when looking at these correlations more broadly, that is on average for the whole gauge ensemble, we see a clear trend: Gribov copies with very small λ_1 tend to yield a larger ghost propagator at low momentum, than copies with large λ_1 (see, e.g., Fig. 2 in [51]). This anti-correlation is smaller the larger the momentum, and is also considerably smaller for the gluon propagator at same momentum.

These correlations are also seen when comparing averaged lattice data as shown in Fig. 3. There the left panels compare the momentum dependence of the $SU(2)$ ghost dressing function (top) and the gluon propagator (bottom) as obtained on first, lowest, highest and best copies of our gauge ensemble (refer to Sect. 2 for this classification). The right panels confront the corresponding data for the strong coupling constant,

$$\alpha_{SU(2)}^{\text{MM}}(p) = \frac{g_0^2(a)}{4\pi} Z(a, p) \cdot J^2(a, p), \quad (3)$$

here in the Minimal MOM scheme for $SU(2)$ Landau gauge [52], and of the inverse renormalization constant \tilde{Z}_1^{-1} of the gh-g1 vertex with zero incoming gluon momentum.

Looking first at the first-copy (*fc*) data points (black open circles in Fig. 3), we see these behave as expected [13, 14, 16, 33, 34]: The ghost dressing function and the gluon propagator increase with decreasing momentum and tend to reach a plateau at very low momentum, while $\alpha_{SU(2)}^{\text{MM}}$ grows with decreasing momentum down to about $a^2 p^2 = 0.2$ ($p \approx 0.5 \text{ GeV}$) below which it falls off again with momentum. Also \tilde{Z}_1^{-1} is found as expected: $\tilde{Z}_1^{-1} \rightarrow 1$ for large momenta, as it should, and for intermediate momenta we see its characteristic hump [39, 40, 53].

But the most interesting data in Fig. 3 is the lowest (*lc*) and highest-copy (*hc*) data (squares and triangles). The *lc* data points, for example, for the ghost dressing function clearly deviate upwards from the respective *hc* data below $a^2 p^2 = 0.5$. Similar is seen for the gluon propagator below $a^2 p^2 = 0.03$. These deviations then yield a coupling, $\alpha_{SU(2)}^{\text{MM}}$, whose running is slightly upwards/downwards shifted below $a^2 p^2 = 0.5$.

Admittedly, compared to the ghost dressing function, the effect for the gluon propagator is small, but we find that it becomes more and more pronounced when increasing statistics.

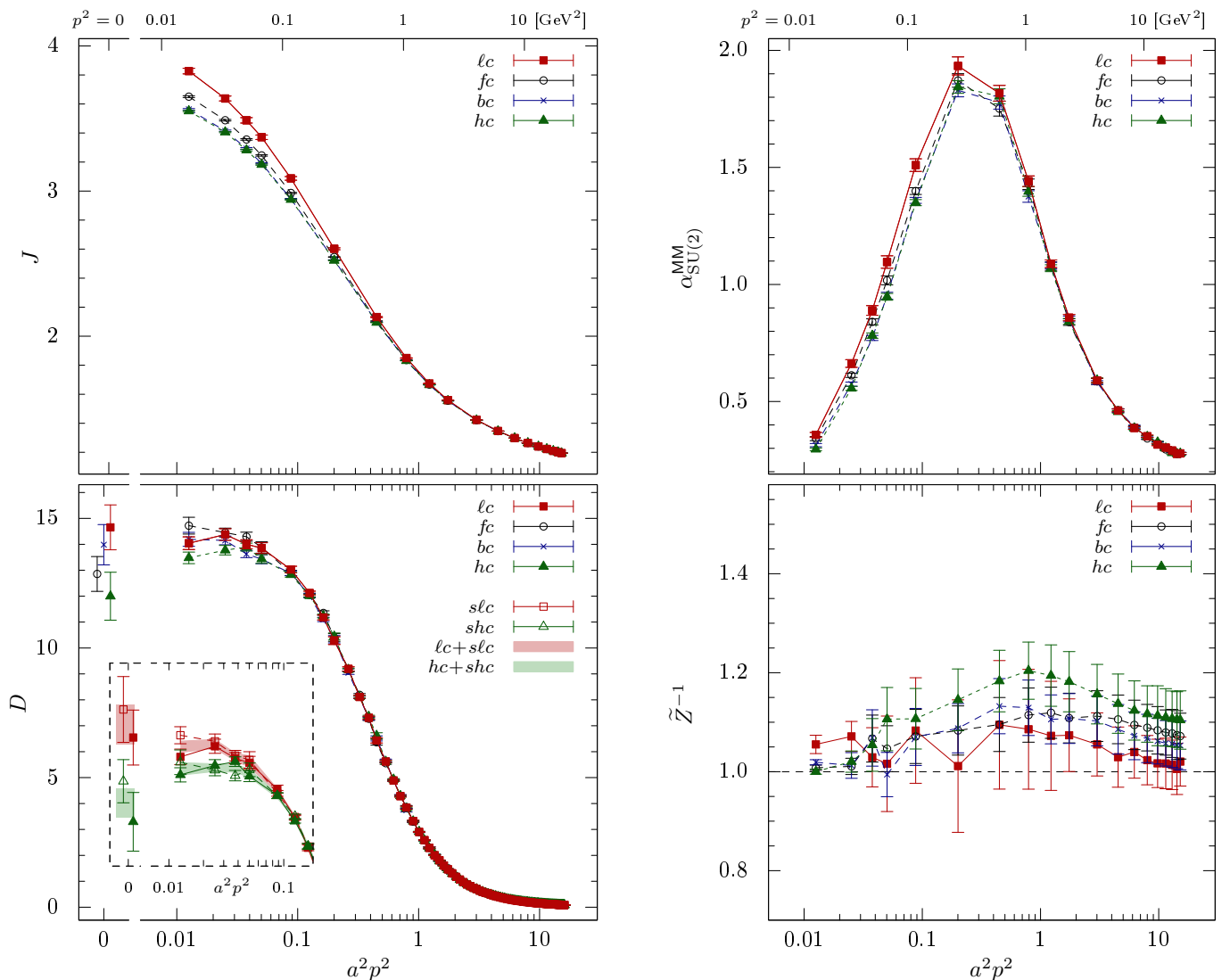


Figure 3: Ghost dressing function (top left), gluon propagator (bottom left), the coupling $\alpha_{\text{SU}(2)}^{\text{MM}}$ (top right) and the inverse renormalization constant of the gh-gl-vertex (bottom right); all versus lattice momentum squared, in lattice units and for SU(2). No renormalization has been applied. Open circles (filled squares, crosses, full triangles) refer to fc (lc , bc , hc) data. The lower left panel also shows a zoomed-in plot to improve visibility of the low-momentum region. This panel also shows slc and shc data. Note the different scales for the x-axis (log and linear) in the left panels and the corresponding physical momenta above the top panels. The $D(0)$ points are slightly shifted to improve visibility.

To cross-check that the λ_1 -dependence we see for the gluon propagator is not just a statistical artifact, we performed additional calculations of the gluon propagator on all Gribov copies with the second lowest and second highest λ_1 . Those additional sets of (2×80) Gribov copies (labeled slc and shc in what follows) are distinct from the sets of lowest and highest copies (lc and hc) analyzed above, and if there is a dependence on λ_1 , one should also see it when comparing slc and shc data. And in fact, also this data clearly exhibits a λ_1 -dependence at low momenta (see zoomed-in plot in Fig. 3). The combined lc and slc data and the combined hc and shc data (colored error bands, same panel) currently gives the best impression of this dependence. Note that such a combination of data is justified, as there are no correlations visible between data from different

copies of the same configuration, and by construction these sets of Gribov copies come also with similar small or large values for λ_1 : The averaged λ_1 values on these four sets of Gribov copies are: $\langle \lambda_1 \rangle_{lc} = 1.43(9) \times 10^{-4}$, $\langle \lambda_1 \rangle_{slc} = 2.14(9) \times 10^{-4}$, $\langle \lambda_1 \rangle_{hc} = 20.33(6) \times 10^{-4}$ and $\langle \lambda_1 \rangle_{shc} = 19.89(4) \times 10^{-4}$, all in lattice units.

So we think the effects we find for both propagators and $\alpha_{\text{SU}(2)}^{\text{MM}}$ are not statistical artifacts, but result from our selection of Gribov copies with respect to λ_1 . A selection based on values for the ghost dressing function, as proposed in [35], would probably result in something similar.

For completeness, we also show the corresponding best-copy (bc) data in Fig. 3 (blue crosses, partly hidden by the hc data). Comparing this with the fc data, we find the expected suppres-

sion of the bc data for the ghost and gluon propagator at low momentum which is then also seen for $\alpha_{\text{SU}(2)}^{\text{MM}}$. Similar was seen for the bc data in [15, 33], although there the effect was even bigger when using the FSA gauge-fixing, a special combination of the simulated annealing and over-relaxation algorithm for gauge-fixing and $Z(2)$ flips, which is most suitable for finding Gribov copies with large $F_U[g]$ values.

Note that the coincidence of the hc and bc data for the ghost dressing functions is likely to be accidentally. For these two sets the dependence on the gauge-functional value (decrease for increasing $F_U[g]$) adds to the dependence on λ_1 (decrease for increasing λ_1). See, once again, Fig. 2 in [51].

For all four types of Gribov copies, we find \tilde{Z}_1^{-1} remains almost unaffected (see lower right panel of Fig. 3). There are small upward shifts for the hc data compared to the ℓc data, but these shifts are all within (statistical) errors. This certainly deserves further study, because at large momenta \tilde{Z}_1 should approach 1 for all types of copies [52, 54], while at small momenta \tilde{Z}_1 is expected to approach 1, or at least a value close to 1 [20].

5. Discussion and Summary

We have demonstrated that the low-momentum behavior of the Landau-gauge gluon and ghost propagators can be changed on the lattice by an additional constraint on the lowest-lying (non-trivial) eigenvalue, λ_1 , of the FP operator. If the lattice Landau gauge fixing is tuned to find Gribov copies with a very small λ_1 , the ghost dressing function gets more enhanced towards the infrared momentum limit, while it rises less steep for large λ_1 . A similar but less pronounced effect is seen for the gluon propagator. Currently the effect for the gluon propagator is best seen if one combines the data from Gribov copies with lowest and second lowest λ_1 , and from copies with highest and second highest λ_1 as shown, e.g., in Figs. 3 or 4. The combined effect of gluon and ghost propagator then yields a coupling constant $\alpha_{\text{SU}(2)}^{\text{MM}}$ whose running changes slightly for momenta below 0.7 GeV.

These Gribov-copy effects are not noticeable at momenta above 1 GeV. Also, these effects cause only a quantitative but no qualitative change of both these propagators at low momentum. Their modified momentum dependences are still of decoupling type. But interestingly, the change we find with λ_1 looks very much alike the change of the gluon and ghost dressing functions, Z and J , with the (boundary) condition on $J(0)$ as found in [22].

To demonstrate this we confront our data for the ghost dressing function and the gluon propagator in Fig. 4 with a corresponding pair of decoupling solutions from [22]⁴. These DSE solutions are approximately those where the boundary condition on the ghost dressing function was set to $J(0) = 3.4$ and $J(0) = 3.8$, respectively. For the comparison our data has been renormalized relatively to the given decoupling solution by applying a common renormalization factor (Z_J and Z_D) to the respective data. Since DSE truncation effects on the solutions

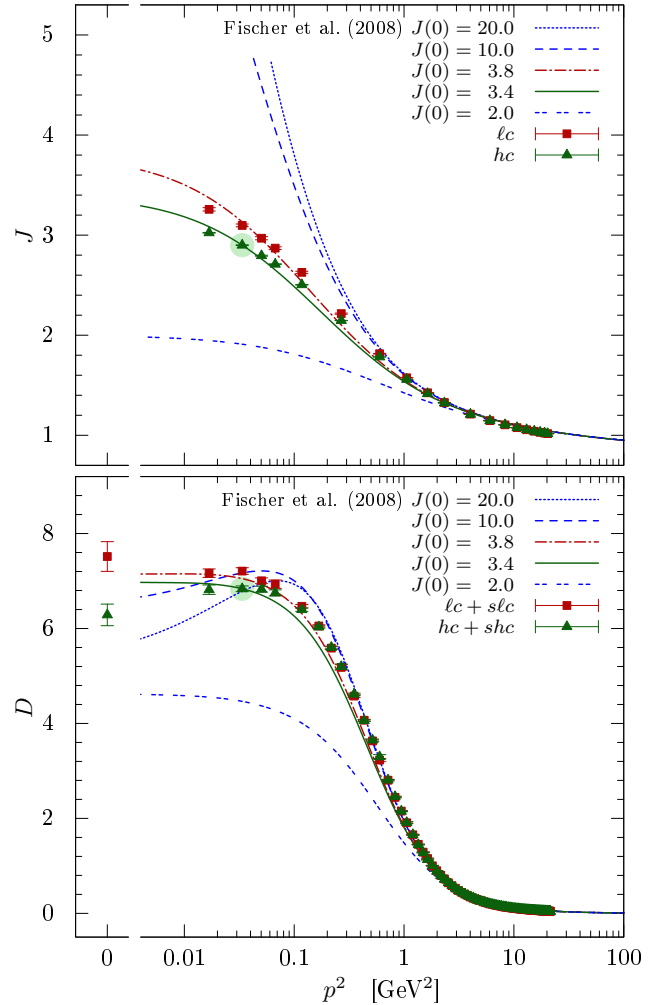


Figure 4: Ghost dressing function (top) and gluon propagator (bottom) versus p^2 . Full symbols refer to our lattice data and lines to five selected decoupling (DSE) solutions from [22]. Note, the order of the gluon propagator lines at low momenta changes somewhere between $J(0) = 3.8$ and 10. The two green-highlighted triangles have been used to fix the relative renormalization factors Z_J and Z_D between the data and the decoupling solutions (see text).

are expected to become important for intermediate (around 1 GeV) and higher momenta, Z_J and Z_D were chosen such that the hc -data points (green triangles) agree with the $J(0) = 3.4$ curves (green) at the second lowest finite momenta (this point is highlighted by green circle in the figure). Of course, one could choose any other point at low p^2 , which would result in a similar figure. But at the moment our comparison is only qualitative anyway.

A more quantitative comparison is possible though, if one looks directly at the strong coupling constant [Eq. (3)]. For this *no* relative renormalization factors are needed and the respective DSE and lattice data should agree, apart from discretization and finite-size effects (for the lattice data) and truncation effects (for the DSE solutions) at intermediate and larger momenta. In Fig. 5 we show such a comparison for the decoupling (DSE) solutions with $J(0) = 3.4$ and 3.8, respectively. The surprisingly good agreement between the propagators and the cou-

⁴The DSE solutions we use here are renormalized such that $\alpha_s^{\text{MM}}(\mu) = 0.3$.

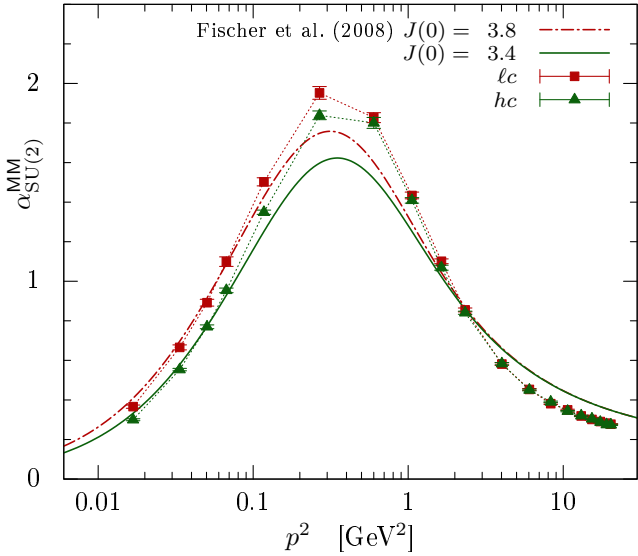


Figure 5: The strong coupling constant [Eq. (3)] versus p^2 . Symbols refer to our lattice data (same as in Fig. 3) and (full/dash-dotted) lines to two selected decoupling solutions from [22].

pling constant at small momenta for the so different approaches to Landau-gauge Yang-Mills theory is encouraging.

Note again that only for small momenta a quantitative agreement can be expected at present. This is primarily due to the used DSE solutions themselves. These were obtained for a truncated system of gluon and ghost DSEs (see [22]) and it is known that these truncations affect the solutions, in particular at intermediate momenta. Also the running of $\alpha_s^{\text{MM}}(p)$ at very large p is only exact up to 1-loop order for these solutions [36]. Improved truncation schemes will however help to reduce the gap between lattice data and DSE solutions in the future (see, e.g., [10] where an improvement has been achieved recently). But to be fair, also our lattice data is not yet perfect: it is for a large ($aL_\mu \approx 9.6\text{fm}$) but still rather coarse lattice and neither infinite-volume nor continuum-extrapolated. That is, the lattice points at larger momenta will slightly deviate from the momentum dependence in the continuum limit.⁵

It is because of the fact that all these effects are less severe for small momenta, why a quantitative agreement should be expected only there.

Nonetheless, with our somewhat exploratory study we primarily focused on the correlation between the FP eigenvalue spectrum and the ghost and gluon propagators, in particular if a change in a constraint on λ_1 is reflected in a *simultaneous* change of the ghost and gluon propagators at low momentum, and if this change qualitatively agrees with [22]. We therefore chose SU(2) and a fixed but rather coarse 56^4 lattice ($\beta = 2.3$) on purpose. It has allowed us to get (with reasonable computer time) data for the gluon propagator and the ghost dressing function where their momentum dependence starts to become flat,

and this for a sufficient number of Gribov copies (at least 200 per configuration) such that a correlation between λ_1 and both propagators could be seen. Also, the use of a single lattice size and spacing has the advantage that one can reveal the effect without having to correct for other effects at the same time (finite volume, lattice spacing, renormalization). It brings, however, the disadvantage that we have no control yet over finite-volume and discretization effects.

For a future study, we therefore suggest to explore how the correlations between the ghost dressing function, the gluon propagator and λ_1 change if the lattice volume is increased and the lattice spacing decreased. This is important, in particular for the gluon propagator whose low-momentum behavior changes only little, if one constrains λ_1 , or $J(0)$ in the continuum. Also 3-point functions of gluon and ghost fields should be checked for this effect, and what changes when adding fermions. Such calculations will however become expensive very quickly—especially, if Gribov copies with exceptionally small or large λ_1 still have to be found by chance. Algorithmic improvements would therefore be quite helpful. For example, a gauge-fixing algorithm that automatically selects Gribov copies with λ_1 values from a given range. For this it may be enough to concentrate first on the less expensive SU(2) gauge group as done here. The gluon and ghost propagators for SU(2) and SU(3) were seen to differ only little [14, 56]; hence no qualitative changes are expected.

One should also check how the distribution of λ_1 (Fig. 1) changes on larger and finer lattices. From [46] and our own study in [49] one would expect that the distribution of λ_1 for random Gribov copies shrinks towards smaller values the larger the lattice size.⁶ If this is also the case for the distribution of λ_1 for all Gribov copies of a single gauge configuration, a distinction between lc and hc copies would be less and less possible. On the other hand, the continuum results of [22, 23] and all currently available lattice results do not indicate that in the infinite-volume limit the Gribov problem disappears and only an infrared diverging ghost dressing function and infrared vanishing gluon propagator remains, as one would expect for $\lambda_1 \rightarrow 0$ from [46]. But this certainly deserves further study.

Let us finally comment on the “rigorous bounds” introduced in [50, 57] to control the infinite-volume extrapolations of lattice data for the gluon and ghost propagator. Since these bounds are composed of the lattice gluon field (for the gluon propagator), and of λ_1 and the eigenmode $\vec{\Phi}_1$ (for the ghost propagator), these will suffer from similar Gribov problems as seen for the propagators here. For a particular lattice implementation of Landau-gauge Yang-Mills theory and a particular selection of Gribov copies these bounds will certainly constrain the lattice data, but one should keep in mind these bounds may change when using other copies or implementations.

Summarizing, with the current (standard) lattice implementation of Landau-gauge Yang-Mills theory, one seems to be able to realize varying decoupling-type solutions for the gluon and

⁵An example of how these deviations look like is given Fig. 2 of [55] for 1-loop lattice perturbation theory.

⁶Though note that in [49] the effect was not analyzed for varying lattice spacings and a fixed lattice volume. And it would also be compatible if only the peak (see Fig. 1) shifts to lower values with increasing volume.

ghost propagators within a small parameter range. This is possible by supplementing the lattice Landau-gauge condition by an additional constraint, as, e.g., the one here or in [35]. But it will perhaps be impossible to find an indication for the scaling solution on a finite lattice. Even if we were able to find for every gauge configuration that Gribov copy with the smallest λ_1 , this eigenvalue and all the others would still be non-zero, i.e., this copy is not on the Gribov horizon. It remains to be seen if for such an approach the scaling behavior can then appear in the limit of infinite volume and zero lattice spacing, as discussed above.

Acknowledgments

This work was supported by the European Union under the Grant Agreement number IRG 256594. We thank C. Fischer, A. Maas and J. Pawłowski for helpful comments and providing partly unpublished data. We acknowledge generous support of computing time from the HLRN (Germany).

References

- [1] R. Alkofer, L. von Smekal, Phys.Rept. 353 (2001) 281. [arXiv:hep-ph/0007355](#).
- [2] J. M. Pawłowski, Annals Phys. 322 (2007) 2831–2915. [arXiv:hep-th/0512261](#).
- [3] H. Gies [arXiv:hep-ph/0611146](#).
- [4] C. S. Fischer, J.Phys. G32 (2006) R253–R291. [arXiv:hep-ph/0605173](#).
- [5] C. Roberts, M. Bhagwat, A. Holl, S. Wright, Eur.Phys.J.ST 140 (2007) 53–116. [arXiv:0802.0217](#).
- [6] A. Maas, Phys.Rept. 524 (2013) 203–300. [arXiv:1106.3942](#).
- [7] P. Boucaud, J. Leroy, A. L. Yaouanc, J. Micheli, O. Pene, et al., Few Body Syst. 53 (2012) 387–436. [arXiv:1109.1936](#).
- [8] C. D. Roberts [arXiv:1203.5341](#).
- [9] C. S. Fischer, A. Maas, J. M. Pawłowski, PoS CONFINEMENT8 (2008) 043. [arXiv:0812.2745](#).
- [10] M. Q. Huber, L. von Smekal [arXiv:1211.6092](#).
- [11] A. Sternbeck, E.-M. Ilgenfritz, M. Müller-Preussker, A. Schiller, Phys.Rev. D72 (2005) 014507. [arXiv:hep-lat/0506007](#).
- [12] P. Boucaud, J. Leroy, A. Le Yaouanc, A. Lokhov, J. Micheli, et al. [arXiv:hep-ph/0507104](#).
- [13] A. Cucchieri, T. Mendes, PoS LAT2007 (2007) 297. [arXiv:0710.0412](#).
- [14] A. Sternbeck, L. von Smekal, D. Leinweber, A. Williams, PoS LAT2007 (2007) 340. [arXiv:0710.1982](#).
- [15] V. Bornyakov, V. Mitrushkin, M. Müller-Preussker, Phys.Rev. D79 (2009) 074504. [arXiv:0812.2761](#).
- [16] I. Bogolubsky, E.-M. Ilgenfritz, M. Müller-Preussker, A. Sternbeck, Phys.Lett. B676 (2009) 69–73. [arXiv:0901.0736](#).
- [17] O. Oliveira, P. Silva, Phys.Rev. D79 (2009) 031501. [arXiv:0809.0258](#).
- [18] J. M. Pawłowski, D. Spielmann, I.-O. Stamatescu, Nucl.Phys. B830 (2010) 291–314. [arXiv:0911.4921](#).
- [19] O. Oliveira, P. J. Silva, Phys.Rev. D86 (2012) 114513. [arXiv:1207.3029](#).
- [20] C. Lerche, L. von Smekal, Phys.Rev. D65 (2002) 125006. [arXiv:hep-ph/0202194](#).
- [21] D. Zwanziger, Phys.Rev. D65 (2002) 094039. [arXiv:hep-th/0109224](#).
- [22] C. S. Fischer, A. Maas, J. M. Pawłowski, Annals Phys. 324 (2009) 2408–2437. [arXiv:0810.1987](#).
- [23] F. J. Llanes-Estrada, R. Williams, Phys.Rev. D86 (2012) 065034. [arXiv:1207.5950](#).
- [24] L. von Smekal, R. Alkofer, A. Hauck, Phys.Rev.Lett. 79 (1997) 3591–3594. [arXiv:hep-ph/9705242](#).
- [25] A. Aguilar, A. Natale, JHEP 0408 (2004) 057. [arXiv:hep-ph/0408254](#).
- [26] P. Boucaud, T. Bruntjen, J. Leroy, A. Le Yaouanc, A. Lokhov, et al., JHEP 0606 (2006) 001. [arXiv:hep-ph/0604056](#).
- [27] D. Dudal, S. Sorella, N. Vandersickel, H. Verschelde, Phys.Rev. D77 (2008) 071501. [arXiv:0711.4496](#).
- [28] A. Aguilar, D. Binosi, J. Papavassiliou, Phys.Rev. D78 (2008) 025010. [arXiv:0802.1870](#).
- [29] P. Boucaud, J.-P. Leroy, A. L. Yaouanc, J. Micheli, O. Pene, et al., JHEP 0806 (2008) 012. [arXiv:0801.2721](#).
- [30] P. Boucaud, J. Leroy, A. Le Yaouanc, J. Micheli, O. Pene, et al., JHEP 0806 (2008) 099. [arXiv:0803.2161](#).
- [31] T. Bakeev, E.-M. Ilgenfritz, V. Mitrushkin, M. Müller-Preussker, Phys.Rev. D69 (2004) 074507. [arXiv:hep-lat/0311041](#).
- [32] I. Bogolubsky, V. Bornyakov, G. Burgio, E. Ilgenfritz, M. Müller-Preussker, et al., Phys.Rev. D77 (2008) 014504. [arXiv:0707.3611](#).
- [33] V. Bornyakov, V. Mitrushkin, M. Müller-Preussker, Phys.Rev. D81 (2010) 054503. [arXiv:0912.4475](#).
- [34] I. Bogolubsky, E.-M. Ilgenfritz, M. Müller-Preussker, A. Sternbeck, PoS LAT2009 (2009) 237. [arXiv:0912.2249](#).
- [35] A. Maas, Phys.Lett. B689 (2010) 107–111. [arXiv:0907.5185](#).
- [36] A. Maas, private communication (2013).
- [37] A. Maas, PoS Confinement X (2013) 034. [arXiv:1301.2965](#).
- [38] R. Lehoucq, K. Maschhoff, D. Sorensen, C. Yang, Arpack software. URL <http://www.caam.rice.edu/software/ARPACK/>
- [39] A. Cucchieri, T. Mendes, A. Mihara, JHEP 0412 (2004) 012. [arXiv:hep-lat/0408034](#).
- [40] A. Sternbeck, The Infrared behavior of lattice QCD Green’s functions, Ph.D. thesis, Humboldt-University Berlin (2006). [arXiv:hep-lat/0609016](#).
- [41] A. Sternbeck, L. von Smekal, Eur.Phys.J. C68 (2010) 487–503. [arXiv:0811.4300](#).
- [42] K. Langfeld, Phys.Rev. D76 (2007) 094502. [arXiv:0704.2635](#).
- [43] I. Bogolubsky, G. Burgio, M. Müller-Preussker, V. Mitrushkin, Phys.Rev. D74 (2006) 034503. [arXiv:hep-lat/0511056](#).
- [44] D. Zwanziger, Nucl.Phys. B412 (1994) 657–730.
- [45] D. Zwanziger, Nucl.Phys. B518 (1998) 237–272.
- [46] D. Zwanziger, Phys.Rev. D69 (2004) 016002. [arXiv:hep-ph/0303028](#).
- [47] D. Zwanziger, Phys.Rev. D67 (2003) 105001. [arXiv:hep-th/0206053](#).
- [48] D. Dudal, J. A. Gracey, S. P. Sorella, N. Vandersickel, H. Verschelde, Phys.Rev. D78 (2008) 065047. [arXiv:0806.4348](#).
- [49] A. Sternbeck, E.-M. Ilgenfritz, M. Müller-Preussker, Phys.Rev. D73 (2006) 014502. [arXiv:hep-lat/0510109](#).
- [50] A. Cucchieri, T. Mendes, Phys.Rev. D78 (2008) 094503. [arXiv:0804.2371](#).
- [51] A. Sternbeck, M. Müller-Preussker, PoS Confinement X (2013) 074. [arXiv:1304.1416](#).
- [52] L. von Smekal, K. Maltman, A. Sternbeck, Phys.Lett. B681 (2009) 336–342. [arXiv:0903.1696](#).
- [53] A. Cucchieri, A. Maas, T. Mendes, Phys.Rev. D77 (2008) 094510. [arXiv:0803.1798](#).
- [54] J. Taylor, Nucl.Phys. B33 (1971) 436–444.
- [55] A. Sternbeck, K. Maltman, M. Müller-Preussker, L. von Smekal, PoS LATTICE2012 (2012) 243. [arXiv:1212.2039](#).
- [56] A. Cucchieri, T. Mendes, O. Oliveira, P. Silva, Phys.Rev. D76 (2007) 114507. [arXiv:0705.3367](#).
- [57] A. Cucchieri, T. Mendes, Phys.Rev.Lett. 100 (2008) 241601. [arXiv:0712.3517](#).